BIOCHEMISTRY
including biophysical chemistry & molecular biology

Article

pubs.acs.org/biochemistry

First Quantum Mechanics/Molecular Mechanics Studies of the Inhibition Mechanism of Cruzain by Peptidyl Halomethyl Ketones

Kemel Arafet, Silvia Ferrer,* and Vicent Moliner*

Departament de Química Física i Analítica, Universitat Jaume I, 12071 Castelló, Spain

Supporting Information

ABSTRACT: Cruzain is a primary cysteine protease expressed by the protozoan parasite *Trypanosoma cruzi* during Chagas disease infection, and thus, the development of inhibitors of this protein is a promising target for designing an effective therapy against the disease. In this paper, the mechanism of inhibition of cruzain by two different irreversible peptidyl halomethyl ketones (PHK) inhibitors has been studied by means of hybrid quantum mechanics/molecular mechanics−molecular dynamics (MD) simulations to obtain a complete representation of the possible free energy reaction paths. These have been traced on free energy surfaces in terms of the potential of mean force computed at AM1d/MM and DFT/MM levels of theory. An analysis of the possible reaction mechanisms of the inhibition process has been performed showing that the nucleophilic attack of an active site cysteine, Cys25, on a carbon atom of the inhibitor and the cleavage of the halogen−carbon bond take place in a single step. PClK appears to be much more favorable than PFK from a kinetic point of view. This result would be in agreement with experimental studies in other papain-like enzymes. A deeper analysis of the results suggests that the origin of the differences between PClK and PFK can be the different stabilizing interactions established between the inhibitors and the residues of the active site of the protein. Any attempt to explore the viability of the inhibition process through a stepwise mechanism involving the formation of a thiohemiketal intermediate and a three-membered sulfonium intermediate has been unsuccessful. Nevertheless, a mechanism through a protonated thiohemiketal, with participation of His159 as a proton donor, appears to be feasible despite showing higher free energy barriers. Our results suggest that PClK can be used as a starting point to develop a proper inhibitor of cruzain.

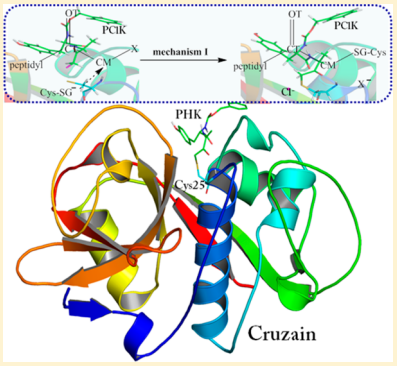

Chagas disease (American trypanosomiasis) is an illness caused by the protozoan parasite *Trypanosoma cruzi* and was discovered in 1909 by the Brazilian doctor Carlos Chagas (1879−1934).[1] It is estimated that the illness affects ∼7−8 million people living mainly in endemic Latin American countries.[2] The movement of Chagas disease to areas previously considered nonendemic, resulting from increasing population mobility between Latin America and the rest of the world, represents a serious public health challenge.[3] There is not any available vaccine to prevent Chagas disease, and the two available drugs for treatment, benznidazole and nifurtimox, are not only toxic and and have important contra-indications (pregnancy, renal or hepatic failure, and psychiatric and neuronal disorders) but also ineffective for the chronic stage of the disease.[4,5] Clearly, there is an urgent need to develop an effective therapy against Chagas disease. One approach consists of developing inhibitors of cruzain, the primary cysteine protease expressed by *T. cruzi* during infection.[6−8]

Cruzain, which belongs to the family of cysteine proteases, was initially discovered from the parasite cell-free extracts and subsequently heterologously expressed in *Escherichia coli*.[9,10] This protease is expressed in all life cycle stages of the parasite and is involved in nutrition and the fight against host defense mechanisms.[11−14] Addition of a cruzain inhibitor to cultures of mammalian cells exposed to trypomastigotes or to mammalian cells already infected with *T. cruzi* amastigotes blocks replication and differentiation of the parasite, thus interrupting the parasite life cycle.[15−21]

Several groups have demonstrated that irreversible inhibition of cruzain by small molecules eradicates infection of the parasite in cell culture and animal models.[17,22−25] Irreversible inhibitors that contain an electrophilic functional group, such as vinyl sulfones, fluoro methyl ketones, aziridines, or nitriles, covalently bind to cruzain via nucleophilic attack of the active site cysteine,[26] showing good inhibition activity.[27,28] In fact, to date, only irreversible inhibitors of cruzain have successfully cured parasitic infection,[23] implying that tight binding to the enzyme may be essential. In this sense, Shoellmann and Shaw developed in 1962 the first peptidyl chloromethyl ketones, L-1-tosyl-amido-2-phenylethyl chloromethyl ketone, as specific inhibitors for the serine protease chymotrypsin.[29] The major disadvantage of this inhibitor was its lack of selectivity because of the great chemical reactivity of the chloroketone functional group. The development of chloromethyl ketone inhibitors led to the investigation of analogous inhibitor structures with different halo leaving groups replacing the chlorine atom. Bromomethyl and iodomethyl ketones have been synthesized

Received: December 22, 2014
Revised: May 7, 2015
Published: May 12, 2015

DOI: 10.1021/bi501551g
Biochemistry 2015, 54, 3381−3391

and are typically more reactive but less stable in aqueous solutions. The first peptide fluoromethyl ketone inhibitors were reported in the literature by Rasnick in 1985[30] and by Shaw's group in 1986.[31] These peptide fluoromethyl ketones were shown to be highly reactive and selective irreversible inhibitors for cysteine proteases. They are poor irreversible inactivators for serine proteases and are not reactive toward bionucleophiles. Inhibition of cruzain activity with fluoromethyl ketone-based inhibitors seems to be correlated with the loss of feasibility of parasites in both *ex vivo* tissue culture and *in vivo* mouse models.[19,32,33]

Information derived from the study of the molecular mechanism of hydrolysis catalyzed by cysteine proteases could be used as a starting point to explore the inhibition mechanism at an atomistic level. Early studies revealed a participation of residues Cys25 and His159 (cruzain numbering) from the active site of these proteases.[34−36] The catalytic cysteine mediates protein hydrolysis via a nucleophilic attack on the carbonyl carbon of a susceptible peptide bond. The imidazole group of the histidine polarizes the SH group of the cysteine and allows deprotonation even at neutral to weakly pH, and a highly nucleophilic thiolate/imidazolium ion pair is thereby produced.[37] The ion pair mechanism explains the unusually high reactivity of cysteine proteases toward electrophilic reagents in comparison to the nucleophilicity of the sulfur of cysteine or glutathione, especially in slightly acidic environments.[38]

With regard to the study of the inhibition mechanism of cysteine proteases, only few irreversible inhibitors have been studied theoretically.[39−46] The study of diazomethyl ketones based on gas phase MNDO calculations proposed a mechanism in which the Cys25 residue binds to the inner diazo nitrogen thus forming an intermediate that evolves to a stable β-thioketone and molecular nitrogen.[44] More recently, density functional theory (DFT) and semiempirical methods have also been used to study the inhibition process of nitrile-containing compounds in the gas phase.[41] Classical MD simulations and exploration of potential energy surfaces (PESs) obtained with quantum mechanics/molecular mechanics (QM/MM) potentials have been used to study the inhibition of cysteine proteases by epoxides and aziridine-based compounds.[42]

Powers and co-workers proposed two possible mechanisms (mechanisms I and II) of irreversible inhibition by peptidyl halomethyl ketones (PHK) based on different crystal structures of cysteine proteases (see Scheme 1).[47] Mechanism I, as shown in Scheme 1, is the direct displacement of the halide group by the thiolate anion. Mechanism II involves formation of a tetrahedral intermediate named thiohemiketal (TH) and a three-membered sulfonium intermediate (TMSI) that rearranges to give the final thioether adduct. The formation of the TH is equivalent to the presence of a tetrahedral intermediate in the serine protease mechanism.[27] Nevertheless, mechanism II has not been supported by theoretical studies. Kollman and co-workers, employing classical molecular mechanics simulations and semiempirical quantum mechanics with model systems to study the cysteine protease catalysis, showed that the attack of S^- on a carbonyl carbon does not involve a stable anionic tetrahedral structure.[48,49] Later, Suhai and co-workers in a QM/MM study of the active site of free papain and of the NMA−papain complex did not obtain a stable tetrahedral NMA−papain complex.[50] Gao and Byun, in a combined QM/MM study of the nucleophilic addition reaction of methanethiolate and *N*-methylacetamide, concluded that there is no stable tetrahedral intermediate in going from the reactant to the tetrahedral adduct.[51] Moreover, Warshel and co-workers in an *ab initio* study of general base/acid-catalyzed thiolysis of formamide and the hydrolysis of methyl thiolformate showed that the anionic tetrahedral intermediate for the acylation reaction was found to be unstable in aqueous solution and to collapse immediately into the neutral form, which is the only intermediate on the reaction pathway.[52] On the basis of DFT methods with model compounds, Kolandaivel and co-workers explored the PESs of the inhibition of haloketones[46] and diketones[43] in the gas phase. According to their results, the thiohemiketal protonated intermediate would be stable but, in general, less stable than the reactant.[43,46] More recently, Zhan and co-workers in a pseudobond first-principles QM/MM-FE study of the reaction pathway for papain-catalyzed hydrolysis of *N*-acetyl-Phe-Gly 4-nitroline concluded that in the acylation step any path that includes the formation of the TH does not exist.[53] Nevertheless, to date, the mechanism of inhibition of cysteine protease by PHKs has not yet been studied by computational tools, including the protein environment effects.

The principal aim of this paper is to gain insights into the mechanism whereby PHK inhibitors bound to a cysteine protease, in particular to cruzain. In a previous theoretical study conducted in our laboratory, the mechanism of inhibition of a protease involved in the degradation of human hemoglobin, namely falcipain-2 (FP2), by the epoxysuccinate *N*-[*N*-(1-hydroxycarboxyethyl-carbony)leucylamino-butyl]guanidine, E64, was conducted.[39] The results indicated that the irreversible attack of a conserved cysteine on E64 can take place on both carbon atoms of its epoxy ring because both processes present similar barriers. We herein present a theoretical study of the

Scheme 1. Reaction Mechanisms of Inhibition of Cysteine Proteases by Peptidyl Halomethyl Ketones (X = F or Cl)[a]

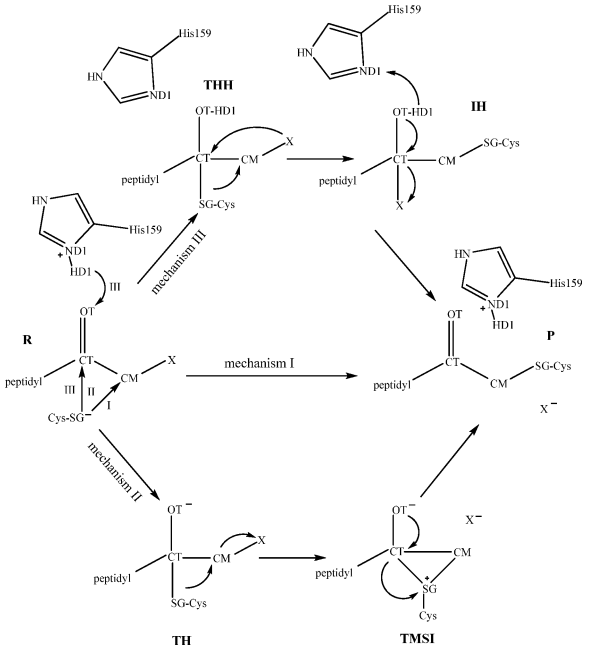

[a]Mechanisms I and II were proposed by Powers and co-workers.[47] TH refers to the thiohemiketal intermediate and TMSI to the three-membered sulfonium intermediate. Mechanism III is an alternative mechanism that takes place through a thiohemiketal protonated intermediate, THH.

DOI: 10.1021/bi501551g
Biochemistry 2015, 54, 3381−3391

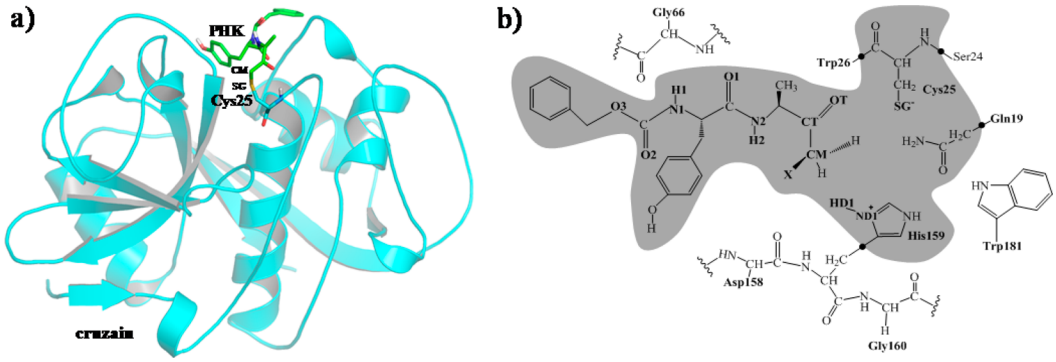

Figure 1. (a) Monomer 1AIM structure showing the crystal structure of cruzain from *T. cruzi* bound to Bz-Tyr-Ala-CH_2F (PFK). The inhibitor (CM) is covalently bound to the enzyme through the SG atom from residue Cys25. The inhibitor and Cys25 are represented as thick sticks. (b) Details of the active site corresponding to the studied model. The gray region corresponds to the QM subset of atoms that includes the inhibitor Bz-Tyr-Ala-CH_2X (X = F or Cl), Cys25, the side chain of Gln19, and the imidazole ring of His159. The link atoms between the QM and MM regions are indicated as black dots.

mechanism of inhibition of cruzain by two PHKs, benzoyl-tyrosine-alanine-fluoromethyl ketone (Bz-Tyr-Ala-CH_2F, or PFK) and benzoyl-tyrosine-alanine-chloromethyl ketone (Bz-Tyr-Ala-CH_2Cl, or PClK). The main difference between these two inhibitors and the previously studied E64 is the presence of the electrophilic functional group, an a halogen atom in PHKs and an epoxide ring and a carboxylic group in E64. The studied proteins belong to the same family of cysteine proteases (clan CA) but are responsible of different human diseases; FP2 is associated with malaria and cruzain with Chagas disease. Hybrid QM/MM[54−56] potentials have been employed to explore the PESs and to run molecular dynamics (MD) simulations that allow the free energy profiles of the reaction to be determined in terms of the potential of mean force (PMF). The reaction mechanisms, with their corresponding free energy barriers, averaged geometries, and interactions between the inhibitor and the protein, have been the subject of a deep analysis that aimed to improve our understanding of the molecular mechanism, paving the way to the design of new inhibitors that allow the effective treatment of Chagas disease.

COMPUTATIONAL MODEL

The initial coordinates were taken from the X-ray crystal structure of cruzain from *T. cruzi* bound to Bz-Tyr-Ala-CH_2F with PDB entry 1AIM[32] at 2.0 Å resolution. The structure consists in one chain of 215 amino acids (cruzain), the inhibitor without the fluor atom, and 46 water molecules (see Figure 1a).

Cruzain is located in the intracellular vesicles during the dormant stage of the parasite at a slighly acidic pH. During the intracellular amastigote stage of the *T. cruzi* life cycle, cruzain is present on the surface of the parasite where the pH of the host cytoplasm is almost neutral (7.4).[32] Thus, hydrogen atoms were added at this physiological pH using the fDYNAMO library,[57] according to the pK_a values of the residues of the 1AIM structure calculated within the empirical PROPKA 3.1 program of Jensen et al.[58−60] Fluor and chlorine atoms were added using Pymol[61] to create the two systems being studied here: Bz-Tyr-Ala-CH_2F and Bz-Tyr-Ala-CH_2Cl. A total of 12 counterions (Na^+) were placed into optimal electrostatic positions around both systems, to obtain electroneutrality. Finally, the systems were placed in a 79.5 Å side cubic box of water molecules.

As depicted in Figure 1b, the inhibitor, Cys25, the side chain of Gln19, and the imidazole ring of His159 (81 atoms) were described by means of the AM1d semiempirical Hamiltonian.[62] Gln19 was treated quantum mechanically to explore its active role in mechanism II, because formation of a bond or charge transfer from the OT atom of the inhibitor must be considered as a possibility. His159 was treated quantum mechanically to explore mechanism III. The rest of the protein and water molecules were described by OPLS-AA[63] and TIP3P[64] force fields, respectively. To saturate the valence of the QM/MM frontier, we used the link atom procedure.[55,65] Because of the size of the full system, all residues more than 25 Å from the CA1 atom of the inhibitor were kept frozen during the simulations (43169 atoms from a total of 50126). A force switch function with a cutoff distance in the range of 14.5−18 Å was applied to treat the nonbonding interactions. All the QM/MM calculations were conducted using the fDYNAMO library.[57]

The two systems were relaxed by means of QM/MM MD for 1 ns at 300 K using the *NVT* ensemble and the Langevin−Verlet integrator. Analysis of the time evolution of the root-mean-square deviation (rmsd) of backbone atoms of the protein and the inhibitor for the Bz-Tyr-Ala-CH_2F and the Bz-Tyr-Ala-CH_2Cl systems confirms that the systems were equilibrated (see Figure S1 of the Supporting Information). Structures obtained after relaxation were used to generate hybrid AM1d/MM PESs. Stationary structures (including reactants, products, intermediates, and transition state structures) were located and characterized by means of a micromacro iterations scheme.[66]

Once the PESs were explored, PMFs generated as a function of a distinguished reaction coordinate (RC) were obtained using the weighted histogram analysis method (WHAM) combined with the umbrella sampling approach.[67,68] The RC is defined depending on the chemical step under study. In general, for the monodimensional PMFs (1D-PMF), the value of the force constant used for the harmonic umbrella sampling was 2500 kJ mol^{-1} $Å^{-2}$ and the simulation windows consisted of equilibration for 20 ps and production for 40 ps, with a time step of 1 fs. Subsequently, 200 ps AM1d/MM MD simulations of the stationary points were performed to analyze the main geometrical parameters as an average. For the study of mechanism I (see Scheme 1), a 1D-PMF AM1d/MM was obtained using the antisymmetric combination of the bond-breaking and bond-forming distances: RC = [d(X−CM) − d(SG−CM)], where X represents F or Cl. This required series of 92 and 85 simulation windows for Bz-Tyr-Ala-CH_2-F and

DOI: 10.1021/bi501551g
Biochemistry 2015, 54, 3381−3391

Bz-Tyr-Ala-CH_2-Cl systems, respectively. For mechanism II (see Scheme 1), a 1D-PMF AM1d/MM was computed to study the formation of the TH from the reactant state using the antisymmetric combination of the bond-breaking and bond-forming distances [RC = d(SG−CT) − d(CT−OT)]. This required series of 61 and 66 simulation windows for Bz-Tyr-Ala-CH_2-F and Bz-Tyr-Ala-CH_2-Cl systems, respectively. A 1D-PMF AM1d/MM was obtained for the formation of the TMSI from the product state using the SG−CT bond-breaking distance as the RC. This required series of 41 and 37 simulation windows for Bz-Tyr-Ala-CH_2-F and Bz-Tyr-Ala-CH_2-Cl systems, respectively. For the study of mechanism III (see Scheme 1), a two-dimensional AM1d/MM PMF (2D-PMF) was computed for the formation of the THH intermediate from the reactant state using the ND1−HD1 bond-breaking distance as RC1 and the SG−CT bond-forming distance as RC2. This required series of 1092 and 1288 simulation windows for Bz-Tyr-Ala-CH_2-F and Bz-Tyr-Ala-CH_2-Cl systems, respectively. For the formation of the IH intermediate from the THH intermediate, an AM1d/MM 2D-PMF was obtained using the SG−CM bond-forming distance as RC1 and the X−CM (X = F or Cl) bond-breaking distance as RC2. This required series of 651 simulation windows for both systems. Finally, a 2D-PMF AM1d/MM was obtained for the formation of the product state from the IH intermediate using the ND1−HD1 bond-forming distance as RC1 and the X−CT (X = F or Cl) bond-breaking distance as RC2. This required series of 1288 and 2310 simulation windows for Bz-Tyr-Ala-CH_2-F and Bz-Tyr-Ala-CH_2-Cl systems, respectively.

Because of the large number of structures that must be evaluated during free energy calculations, QM/MM calculations are usually restricted to the use of semiempirical Hamiltonians. To correct the low-level AM1d energy function used in the 1D-PMFs, an interpolated correction scheme developed in our laboratory has been applied.[69] In this correction scheme, on the basis of a method proposed by Truhlar et al. for dynamical calculations of gas phase chemical reactions,[70] the new energy function employed in the simulations is defined as

$$E = E_{\mathrm{LL/MM}} + S[\Delta E_{\mathrm{LL}}^{\mathrm{HL}}(\zeta)] \quad (1)$$

where S denotes a spline function, whose argument $\Delta E_{\mathrm{LL}}^{\mathrm{HL}}(\zeta)$ is a correction term taken as the difference between single-point calculations of the QM subsystem using a high-level (HL) method and the low-level (LL) one. The correction term is expressed as a function of the distinguished reaction coordinate ζ (RC). When corrections were made on 2D-PMF, the correction term was then expressed as a function of the two coordinates, ζ_1 and ζ_2, to generate the higher-level 2D-PMF. The HL calculations were conducted by means of the M06-2X functional[71] with the 6-31+G(d,p) basis set[72] following the suggestions of Truhlar and co-workers.[71,73] The 6-311+G(2df,2p) basis set[74,75] was also checked for the F system (mechanism I), because this is the one specifically recommended for this element. Tests of the use of both basis sets rendered almost quantitatively equivalent results (see Figure S2 of the Supporting Information), and consequently, the 6-31+G(d,p) basis set was used for all calculations. These calculations were conducted using *Gaussian09*.[76]

RESULTS AND DISCUSSION

The first proposed mechanism of inhibition of cruzain by the two studied PHKs (mechanism I in Scheme 1)[47] has been initially explored by computing the PESs. Once the stationary points were located on the PESs, the mechanisms of both systems were clearly identify as single-step mechanisms, where the attack of Cys25 on carbon CM takes place concomitantly with the breaking of the bond of the halogen with CM.

In the next step, the free energy profiles have been calculated in terms of 1D-PMFs at the AM1d/MM level (see Figure S3 of the Supporting Information) and corrected at the M06-2X/6-31+G(d,p)/MM level (Figure 2). The first observation is the

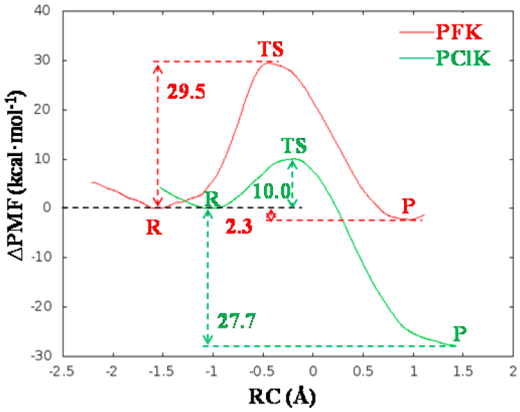

Figure 2. Free energy profiles of cruzain inhibition with PHKs for mechanism I, computed at the M06-2X/6-31+G(d,p)/MM level. RC corresponds to d(X−CM) − d(SG−CM), where X is F (red) or Cl (green).

dramatic influence of increasing the level of the QM region description on the energy barriers and reaction energies. This result justifies the use of high-level Hamiltonians to properly describe the energetics of this chemical reaction when studied by means of QM/MM methods. Consequently, the analysis of energies will be conducted with M06-2X/MM results. As observed in Figure 2, the free energy barrier for the inhibition of cruzain with PClK (∼10 kcal mol^{-1}) is much lower than that obtained with PFK (∼29.5 kcal mol^{-1}). This result would describe a higher chemical reactivity of the peptide inhibitor with cloro than with fluor atoms. Despite no experimental kinetic data being available for the inhibition of cruzain with PHKs, experimental studies with cathepsin B (papain-like enzymes known as clan CA)[77] concluded the reactivity of a PClK is higher than that of a PFK,[27,30,31] in agreement with our results.

Analysis of the reaction energies obtained for both inhibitors shows that the process with PClK appears to be much more exergonic than the reaction with the PFK. Nevertheless, the reaction is irreversible in any case because the leaving anion will diffuse into the surrounding water shell because of the concentration gradients. Quantitative differences in reaction free energies obtained from the PMFs can be due to the limits of the distinguished reaction coordinate that, obviously, do not cover the full diffusion process of the anion into the bulk solvent. Interestingly, and as can be confirmed by the averaged values of the key distances reported in Table 1, the transition state in the PClK system appears at a more advanced value of the RC (−0.09 Å) than in the reaction of PFK (−0.48 Å). The fact that a more advanced TS was not associated with a higher activation barrier is due to the differences observed in the reactant complex: the minimum obtained in the PFK is located at a value of the RC (−1.60 Å) more negative than in the PClK

DOI: 10.1021/bi501551g
Biochemistry 2015, 54, 3381−3391

Table 1. Averaged Distances for Key States Located along the Inhibition of Cruzain by PHK, through Direct Mechanism I[a]

	d (Å)		
	R	TS	P
	(a) PFK		
SG−CM	3.15 ± 0.03	2.52 ± 0.03	1.79 ± 0.03
F−CM	1.55 ± 0.02	2.04 ± 0.03	2.70 ± 0.02
F−H1	4.58 ± 0.11	3.03 ± 0.14	2.55 ± 0.12
F−H2	3.18 ± 0.13	3.41 ± 0.15	6.24 ± 0.91
F−H (H_2O)	4.67 ± 0.99	3.81 ± 1.30	1.52 ± 0.09
F−H (H_2O)	4.23 ± 0.90	3.82 ± 0.74	1.75 ± 0.51
SG−H (Trp26)	1.54 ± 0.14	1.55 ± 0.20	3.15 ± 0.22
SG−H (Gly160)	3.10 ± 0.65	3.56 ± 0.81	2.63 ± 0.24
SG−HD1 (His159)	5.00 ± 0.38	3.17 ± 0.99	4.12 ± 0.28
OT−H (Cys25)	4.74 ± 0.40	5.46 ± 1.13	3.07 ± 0.35
OT−H (Gln19)	6.12 ± 0.82	7.75 ± 1.05	2.93 ± 0.47
O1−H (Trp26)	3.89 ± 0.29	3.94 ± 0.41	1.59 ± 0.23
O1−H (Gly66)	2.22 ± 0.19	5.55 ± 0.43	3.80 ± 0.40
N2−H (Trp26)	5.44 ± 0.24	4.09 ± 0.44	3.49 ± 0.34
N1−H (Gly66)	3.49 ± 0.31	5.23 ± 0.28	2.68 ± 0.40
H2−O (Gly66)	5.37 ± 0.25	2.18 ± 0.31	2.19 ± 0.67
H1−O (Gly66)	2.04 ± 0.24	3.58 ± 0.26	5.60 ± 0.54
	(b) PClK		
SG−CM	2.80 ± 0.03	2.33 ± 0.03	1.78 ± 0.03
Cl−CM	1.77 ± 0.03	2.24 ± 0.03	3.10 ± 0.03
Cl−HD1 (His159)	3.50 ± 0.59	4.06 ± 0.36	2.40 ± 0.20
Cl−HE1 (Trp181)	5.10 ± 0.78	5.76 ± 0.62	3.78 ± 0.76
Cl−H (H_2O)	3.91 ± 0.73	3.36 ± 0.74	2.50 ± 0.26
SG−H (Trp26)	2.38 ± 0.54	2.95 ± 0.29	3.08 ± 0.20
SG−H (His159)	1.92 ± 0.10	5.14 ± 0.29	3.26 ± 0.46
SG−H (Gly160)	2.92 ± 0.66	2.51 ± 0.21	3.03 ± 0.43
OT−H (Cys25)	4.38 ± 0.98	2.55 ± 0.32	3.07 ± 0.64
OT−H (Gln19)	5.74 ± 1.69	2.54 ± 0.33	3.90 ± 0.82
O1−H (Gly66)	3.34 ± 0.73	3.58 ± 0.44	3.92 ± 0.36
O1−H (Trp26)	2.59 ± 1.15	1.65 ± 0.31	1.52 ± 0.20
O2−H (Gly66)	4.42 ± 0.45	2.99 ± 0.45	4.13 ± 0.29
O3−H (Gly66)	3.46 ± 0.68	2.99 ± 0.45	3.01 ± 0.42
N1−H (Gly66)	3.03 ± 0.38	2.74 ± 0.22	2.82 ± 0.24
H1−O (Gly66)	2.01 ± 0.23	2.06 ± 0.20	1.99 ± 0.17
H2−O (Asp158)	3.67 ± 0.47	3.21 ± 0.49	3.43 ± 0.38

[a]Results were obtained from 200 ps AM1d/MM MD simulations on the stationary points taken from the M06-2X/6-31+G(d,p)/MM free energy profiles (in angstroms). Interatomic distances associated with the RCs were constrained during the simulations.

(−1.03 Å). Interestingly, the change in the RC from the reactant complex to the transition state in both systems is very similar [$\Delta RC_{(R,TS)}$ values of 0.94 and 1.12 Å for PClK and PFK, respectively]. Then, the differences in the free energies of activation can not be completely discussed in these terms, and further analysis of average structures of stationary points of the free energy surfaces has to be conducted. Representative snapshots of reactants, transition states, and products of both inhibitory reactions are presented in Figure 3. As observed in the figure, and quantitatively confirmed by the geometrical data listed in Table 1, more hydrogen bond interactions between the inhibitor and the residues of the active site are detected in the TS of PClK (OT−H_{Cys25}, O1−H_{Trp26}, and H1−O_{Gly66}) than in the TS of PFK (H2−O_{Gly66}), which is in agreement with the lower barrier obtained for the former reaction. The larger amount of favorable inhibitor−protein interactions obtained in products of the PClK than in the products of the PFK inhibitor would also support a higher level of stabilization of the PClK−protein complex (see Table 1). The halogen atoms in products appear to be stabilized mainly by interactions with water molecules, in both reactions. It can be observed that fluor ion interacts with a hydrogen H2 atom of the inhibitor and two water molecules. In the case of PClK, chlorine ion interacts, mainly, with His159 and two water molecules but also exhibits weak interactions with Gln19 and Trp181. Thus, the thioether adduct (products) presents interactions that are stronger than those of the reactants, supporting a description as an irreversible inhibition.

As mentioned in the introductory section, Powers and co-workers[47] proposed a second mechanism of inhibition of cruzain by PHKs (mechanism II in Scheme 1) involving the formation of a thiohemiketal intermediate (TH) and a three-membered sulfonium intermediate (TMSI). Nevertheless, all the attempts conducted to explore the mechanism by means of AM1d/MM PESs were unsuccessful. TH has not been found to be a stable intermediate in the PES. This has been confirmed when exploring the evolution of the PMF from reactants to the TH using the d(SG−CT) − d(CT−OT) antisymmetric combination as a reaction coordinate. The resulting PMFs obtained for both inhibitors at the M06-2X/6-31+G(d,p)/MM level (see Figure 4) confirm the instability of the proposed TH. The corresponding profiles at the AM1d/MM level, reported in Figure S4 of the Supporting Information, render the same conclusions.

The minimum that appears in Figure 4a at an RC value of 1.17 Å corresponds to an intermediate with SG−CT and SG−CM distances equal to 2.41 ± 0.03 and 3.06 ± 0.10 Å, respectively. Obviously, this structure does not correspond to the TH. Moreover, further attempts to explore mechanism II were based on the exploration of the step from products to the TMSI. The PMFs obtained as a function of the SG−CT distance render profiles that do not allow the localization of stable structures for this intermediate, as shown in Figure 5. The corresponding profiles at the AM1d/MM level (Figure S5 of the Supporting Information) render the same conclusions. Finally, any attempt to equilibrate the PHK−cruzain systems at TH or TMSI intermediates by means of constrained QM/MM MD simulations reveals the instability of these structures as soon as all atoms of the system are allowed to move (see Figures S6−S8 of the Supporting Information).

These results suggest that inhibition of cruzain by PHKs cannot take place through the proposed mechanism II, a conclusion that is in agreement with previous theoretical studies of different systems showing that the attack of S^- on a C=O bond does not involve a stable anionic tetrahedral structure.[48−53] Moreover, regardless, experimental studies suggest the possibility of mechanism II taking place in serine proteases through the formation of the TH between the serine−OH and C=O bonds from the inhibitor;[78] no experimental evidence of this mechanism in cysteine proteases exists.

Finally, a third mechanism through a protonated thiohemiketal, THH (mechanism III in Scheme 1), has been explored. From a computational point of view, this mechanism appears to be more complex because of the participation of an acid, His159, that protonates the OT carbonyl oxygen of the inhibitor. Consequently, and as described in Computational Model, 2D-PMFs were computed to unequivocally define the mechanism. Thus, the first step corresponds to the attack of

DOI: 10.1021/bi501551g
Biochemistry 2015, 54, 3381−3391

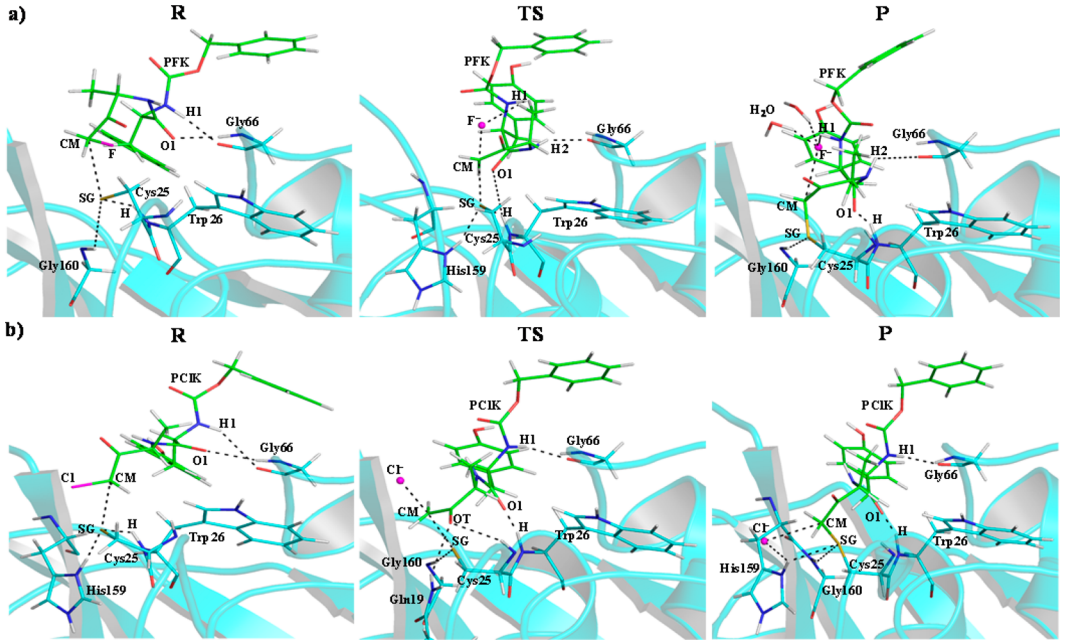

Figure 3. Representative snapshots of the key states of reaction mechanism I of inhibition of cruzain by (a) PFK and (b) PClK.

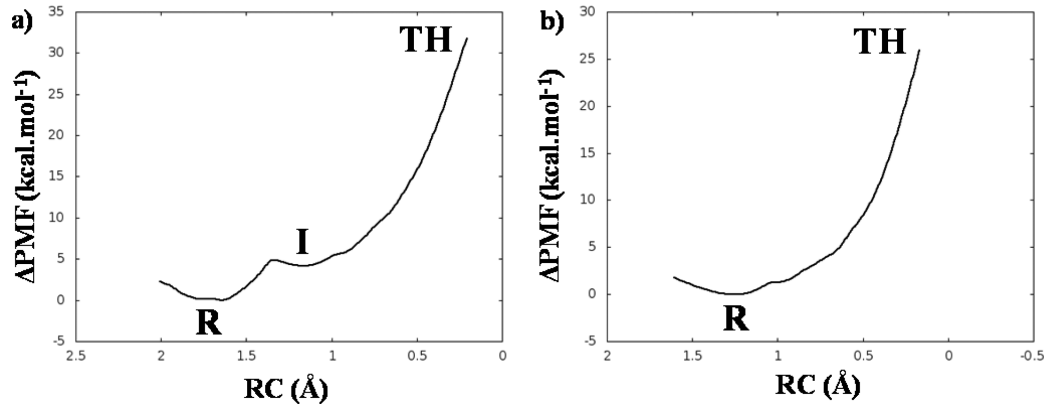

Figure 4. PMFs for the formation of the TH intermediate from reactants computed at the M06-2X/6-31+G(d,p)/MM level: (a) Bz-Tyr-Ala-CH_2F inhibitor and (b) Bz-Tyr-Ala-CH_2Cl inhibitor. RC corresponds to d(SG−CT) − d(OT−CT).

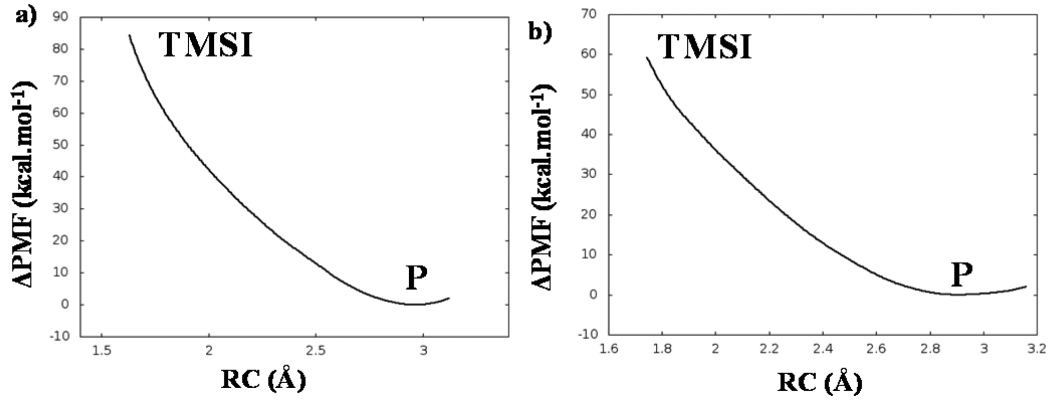

Figure 5. PMFs for the formation of the TMSI intermediate from products, computed at the M06-2X/6-31+G(d,p)/MM level: (a) Bz-Tyr-Ala-CH_2F inhibitor and (b) Bz-Tyr-Ala-CH_2Cl inhibitor. RC corresponds to the d(SG−CT) distance.

Cys25 on the CM carbon atom and the transfer of a proton from His159 to the OT oxygen leading to THH. The resulting FESs obtained at the M06-2X/6-31+G(d,p)/MM level are shown in Figure 6. The corresponding surfaces at the AM1d/MM level are shown in Figure S9 of the Supporting Information. The first conclusion derived from Figure 6 is that this step takes place without any barrier when inhibition takes place with PClK. In the case of PFK, the proton from

DOI: 10.1021/bi501551g
Biochemistry 2015, 54, 3381−3391

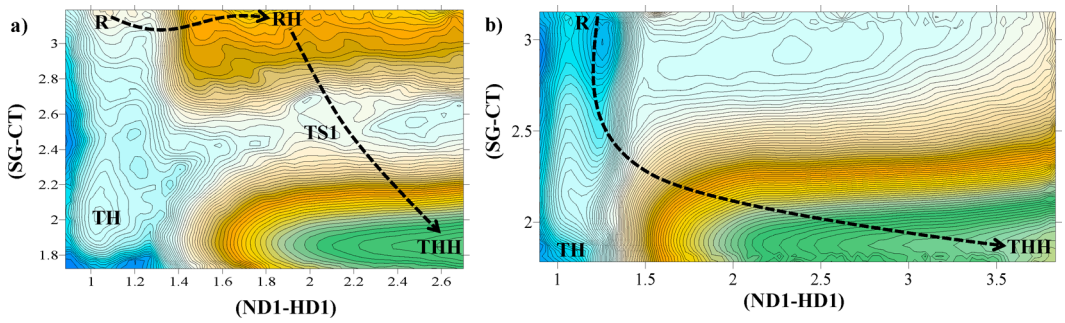

Figure 6. 2D-PMFs for the formation of the protonated thiohemiketal intermediate, THH, from reactants, computed at the M06-2X/6-31+G(d,p)/MM level: (a) Bz-Tyr-Ala-CH_2F inhibitor and (b) Bz-Tyr-Ala-CH_2Cl inhibitor. Distances are in angstroms, and isoenergetic lines are displayed every 0.5 kcal mol^{-1}.

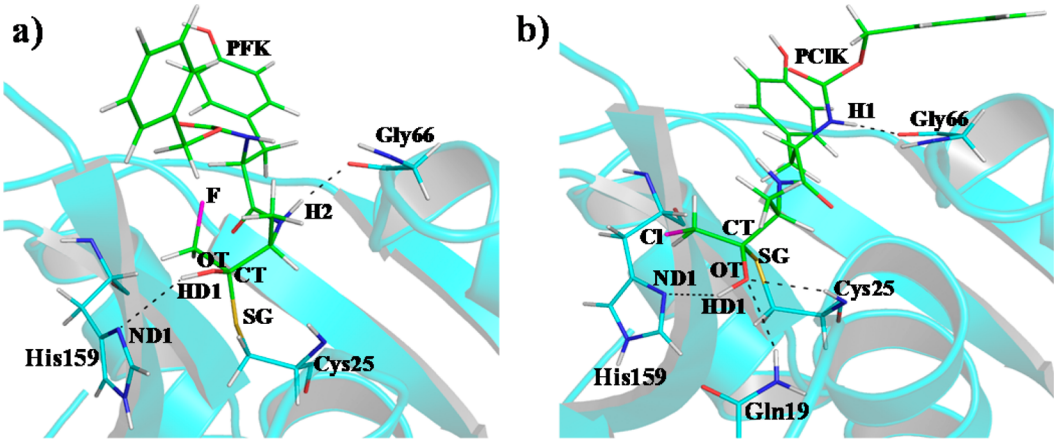

Figure 7. Representative snapshots of the protonated thiohemiketal intermediate, THH, in reaction mechanism III of inhibition of cruzain by (a) PFK and (b) PClK.

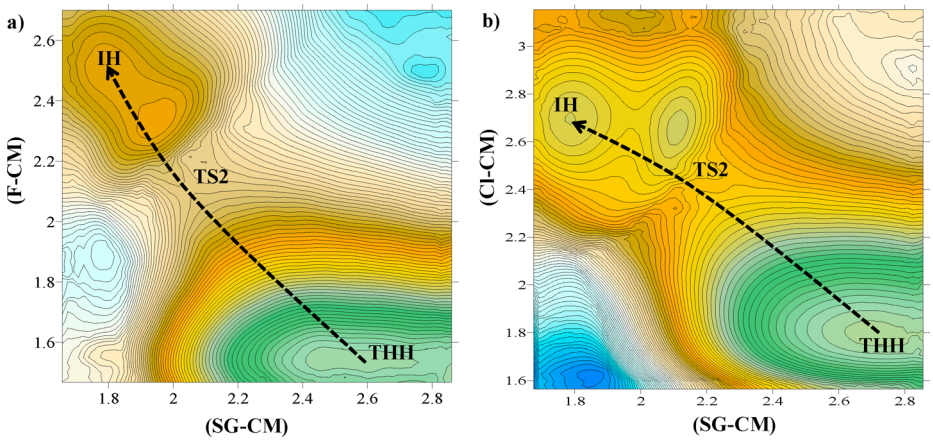

Figure 8. 2D-PMFs for the transformation from protonated thiohemiketal, THH, to intermediate IH, computed at the M06-2X/6-31+G(d,p)/MM level: (a) Bz-Tyr-Ala-CH_2F inhibitor and (b) Bz-Tyr-Ala-CH_2Cl inhibitor. Distances are in angstroms, and isoenergetic lines are displayed every 1.0 kcal mol^{-1}.

His159 is transferred to the OT atom of the inhibitor also without an energy barrier, but rendering a stable intermediate (RH in Figure 6a). Then, the attack of Cys25 on the CT atom proceeds with a free energy barrier defined by TS1. Interestingly, both 2D-PMFs show the protonated thiohemiketal, THH, as a stable species and confirm the previous results (see Figure 4) that indicated the instability of the TH. Representative snapshots of this THH species obtained with both inhibitors are shown in Figure 7.

The second step has also been explored by means of 2D-PMFs, controlling the X−CM and SG−CM distances. The resulting M06-2X/6-31+G(d,p)/MM FESs are presented in Figure 8 (the corresponding surfaces at the AM1d/MM level are shown in Figure S10 of the Supporting Information). In this step, the mechanisms of both inhibitors proceed in an almost equivalent way. Finally, when the last step of the inhibition of cysteine protease by PFK and PClK inhibitors is explored, differences are found. Via comparison of panels a and b of Figure 9, we observed how the transformation from IH to

DOI: 10.1021/bi501551g
Biochemistry 2015, 54, 3381−3391

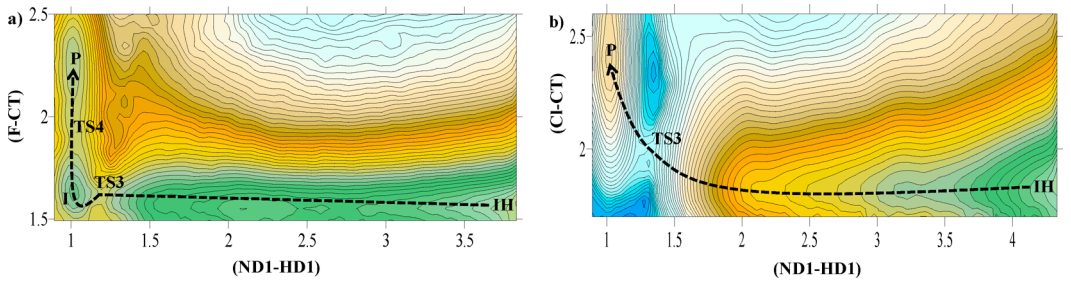

Figure 9. 2D-PMFs for the formation of products from the IH intermediate computed at the M06-2X/6-31+G(d,p)/MM level: (a) Bz-Tyr-Ala-CH_2F inhibitor and (b) Bz-Tyr-Ala-CH_2Cl inhibitor. Distances are in angstroms, and isoenergetic lines are displayed every 1.0 kcal mol^{-1}.

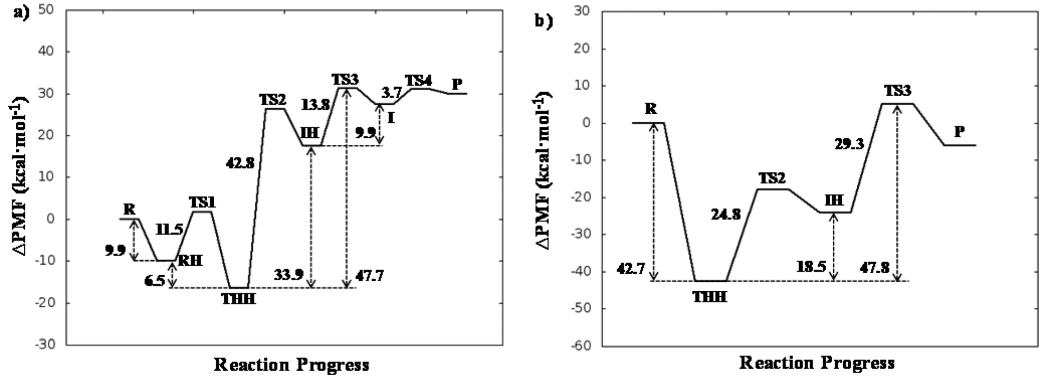

Figure 10. Free energy profiles for the inhibition of cruzain via mechanism III computed at the M06-2X/6-31+G(d,p)/MM level: (a) Bz-Tyr-Ala-CH_2F inhibitor and (b) Bz-Tyr-Ala-CH_2Cl inhibitor.

products takes place in a concerted way for PClK but through a stable intermediate, I, for PFK. The same conclusions are derived form the AM1d/MM free energy surfaces reported in Figure S11 of the Supporting Information.

The complete free energy profiles for the inhibition of cruzain through mechanism III, derived from the M06-2X/MM 2D-PMFs reported in Figures 6, 8, and 9, are summarized in Figure 10. We can conclude that, as was observed for mechanism I, the inhibition of cruzain with PClK is much more favorable than the inhibition with PFK, once again in agreement with experimental studies of papain-like enzyme studies,[77] leading to the conclusion that the reactivity of a PClK is higher than that of a PFK.[27,30,31] The rate-limiting step of mechanism III would correspond to TS3 for both inhibitors with effective free energy barriers, computed from the stabilized THH, of 47.7 and 47.8 kcal mol^{-1} for PFK and PClK, respectively. Nevertheless, as observed on the profiles, if reactants are considered to be the reference state, the inhibition of cruzain with PClK is clearly more feasible than the inhibition with PFK.

From a thermodynamic point of view, the energetic results derived from the FESs in this mechanism would describe an endorgenic process in which inhibition takes place with PFK but an exergonic one for the reaction with the PClK. Regardless, as mentioned above, the reaction must be irreversible because the leaving anion will diffuse into the surrounding water shell because of the concentration gradients. Quantitative differences obtained from the PMFs can be associated with the limits of the distinguished reaction coordinate in the last step that, obviously, do not cover the full diffusion process of the leaving anion.

Analysis of geometries of stationary point structures (reported in Table S1 of the Supporting Information) reveals more hydrogen bond interactions between the inhibitor and the residues of the active site in TS3 of PClK than in TS3 of PFK, which is in agreement with the lower energies obtained for the former reaction. Again, and as observed in the results of mechanism I, the larger amount of favorable inhibitor−protein interactions obtained in products of the PClK compared to the amount in the products of the PFK inhibitor is in agreement with the higher level of stabilization of the PClK−protein complex (see Table S1 of the Supporting Information).

■ CONCLUSIONS

This paper reports the theoretical study of the inhibition of cruzain by two irreversible peptidyl halomethyl ketones inhibitors, Bz-Tyr-Ala-CH_2F (PFK) and Bz-Tyr-Ala-CH_2Cl (PClK), conducted by means of MD simulations using hybrid AM1d/MM and M06-2X/MM potentials. The reaction mechanisms previously proposed in the literature[47] have been explored. According to our results, the nucleophilic attack of the unprotonated Cys25 on the CM atom of the inhibitor (PFK or PClK) and the cleavage of the halogen−CM bond take place in a concerted way. Analysis of free energy barriers and reaction free energies, computed at both levels of theory, shows that the inhibition by PClK would be kinetically and thermodynamically more favorable. In fact, the difference between the barriers of both reactions is ∼3-fold (10.0 and 29.5 kcal mol^{-1} for PClK and PFK, respectively), and even larger differences are obtained upon comparison of the reaction energies stabilized (−27.7 and −2.3 kcal mol^{-1} for PClK and PFK, respectively). It is important to point out that the use of a semiempirical Hamiltonian to treat those atoms described quantum mechanically in our QM/MM scheme provokes an important overestimation of the free energy barriers, by comparison with those generated by DFT methods. Our

DOI: 10.1021/bi501551g
Biochemistry 2015, 54, 3381−3391

results confirm the great chemical reactivity of PClK as an irreversible inhibitor of cruzain. Despite the fact that no experimental kinetic data are available for this particular reaction, our results would be in agreement with experimental studies of other papain-like enzymes (cathepsin B) that concluded that the reactivity of a PClK is higher than that of a PFK. A deeper analysis of the results suggests that the origin of these differences can be in the different stabilizing interactions established between the inhibitors and the residues of the active site of the protein. Any attempt to explore the viability of the inhibition process through a stepwise mechanism involving the formation of a thiohemiketal intermediate and a three-membered sulfonium intermediate has been unsuccessful. All QM/MM calculations show that these intermediates are unstable, which does not lead to recommending the use of the intermediate as a template to design an efficient inhibitor. Nevertheless, an alternative stepwise mechanism has been determined through a protonated thiohemiketal intermediate. This species, which is generated though the transfer of a proton from a histidine residue located in the active site of cruzain protein, His159, and the attack of Cys25 on the CT atom of the inhibitor, appears to be dramatically stabilized with respect to the initial reactant species. Our results suggest that, in fact, this covalently bound inhibitor−protein complex could be a final state of the inhibition process because significant barriers are obtained in going from this complex to the final product complex.

Altogether, our results suggest that benzoyl-tyrosine-alanine-chloromethyl ketone is a good candidate for the development of a proper inhibitor of cruzain, which in turn could be used in the treatment of Chagas desease.

■ ASSOCIATED CONTENT

Supporting Information

Time evolution of the root-mean-square deviation along the QM/MM MD simulation for the backbone atoms of the protein (red line) and atoms of the inhibitor (blue line) for both systems (Figure S1), 1D-PMFs for inhibition of cruzain by PFK through mechanism I at the M06-2X/MM level with 6-31+G(d,p) and 6-311+G(2df,2p) basis sets (Figure S2), AM1d/MM 1D-PMFs of the inhibition of cruzain by PHKs through mechanism I (Figure S3), AM1d/MM 1D-PMFs of the formation of the TH intermediate from reactants for both inhibitors (Figure S4), AM1d/MM 1D-PMFs of the formation of the TMSI intermediate from products for both inhibitors (Figure S5), time-dependent evolution of selected distances on the QM/MM MD simulation corresponding with the TH of both inhibitors (Figure S6), time-dependent evolution of selected distances on the QM/MM MD simulation corresponding with the TMSI of the Bz-Tyr-Ala-CH_2F inhibitor (Figure S7), time-dependent evolution of selected distances on the QM/MM MD simulation corresponding with the TMSI of the Bz-Tyr-Ala-CH_2Cl inhibitor (Figure S8), AM1d/MM 2D-PMFs for the formation of the THH intermediate from reactants for both inhibitors (Figure S9), AM1d/MM 2D-PMFs for the formation of the IH intermediate from THH for both inhibitors (Figure S10), AM1d/MM 2D-PMFs for the formation of P from the IH intermediate for both inhibitors (Figure S11), and averaged distances for key states located along the inhibition of cruzain by PHK, through a mechanism III (Table S1). The Supporting Information is available free of charge on the ACS Publications website at DOI: 10.1021/bi501551g.

■ AUTHOR INFORMATION

Corresponding Authors

*E-mail: sferrer@uji.es. Phone: +34964728084.

*E-mail: moliner@uji.es.

Funding

We thank the FEDER Spanish Ministerio de Economía y Competitividad for Project CTQ2012-36253-C03-01, Generalitat Valenciana for the PrometeoII/2014/022 project, and Universitat Jaume I for Project P11B2014-26. K.A. thanks the Spanish Ministerio de Economía y Competitividad for a predoctoral contract.

Notes

The authors declare no competing financial interest.

■ ACKNOWLEDGMENTS

We acknowledge the Servei d'Informatica, Universitat Jaume I, for a generous allotment of computer time.

■ ABBREVIATIONS

1D, monodimensional; 2D, bidimensional; E64, *N*-[*N*-(1-hydroxycarboxyethyl-carbony)leucylamino-butyl]guanidine; FP2, falcipain-2; HL, high-level; LL, low-level; MD, molecular dynamics; OPLS-AA, optimized potential for liquid simulations of the all-atom force field; PClK, benzoyl-tyrosine-alanine-chloromethyl ketone; PDB, Protein Data Bank; PES, potential energy surface; FES, free energy surface; PFK, benzoyl-tyrosine-alanine-fluoromethyl ketone; PHK, peptidyl halomethyl ketones; PMF, potential of mean force; QM/MM, quantum mechanics/molecular mechanics; QM/MM-FE, quantum mechanics/molecular mechanics free energy; RC, reaction coordinate; rmsd, root-mean-square deviation; TIP3P, transferable intermolecular potential 3P; TH, thiohemiketal; RH, stable intermediate; THH, protonated thiohemiketal; IH, protonated intermediate; I, unprotonated intermediate; TMSI, three-membered sulfonium intermediate; WHAM, weighted histogram analysis method.

■ REFERENCES

(1) Clayton, J. (2010) Chagas disease 101. *Nature 465*, S4−S5.

(2) http://www.who.int/mediacentre/factsheets/fs340/en (2014).

(3) Jackson, Y., Angheben, A., Carrilero Fernandez, B., Jansa i Lopez del Vallado, J. M., Jannin, J. G., and Albajar-Vinas, P. (2009) Management of Chagas disease in Europe. Experiences and challenges in Spain, Switzerland and Italy. *Bull. Soc. Pathol. Exot. Ses Fil. 102*, 326−329.

(4) Castro, J. A., de Mecca, M. M., and Bartel, L. C. (2006) Toxic side effects of drugs used to treat Chagas' disease (American trypanosomiasis). *Hum. Exp. Toxicol. 25*, 471−479.

(5) Filardi, L. S., and Brener, Z. (1987) Susceptibility and natural-resistance of *Trypanosoma cruzi* strains to drugs used clinically in Chagas disease. *Trans. R. Soc. Trop. Med. Hyg. 81*, 755−759.

(6) McKerrow, J. H., Engel, J. C., and Caffrey, C. R. (1999) Cysteine protease inhibitors as chemotherapy for parasitic infections. *Bioorg. Med. Chem. 7*, 639−644.

(7) McKerrow, J. H., McGrath, M. E., and Engel, J. C. (1995) The cysteine protease of *Trypanosoma cruzi* as a model for antiparasite drug design. *Parasitol. Today 11*, 279−282.

(8) Renslo, A. R., and McKerrow, J. H. (2006) Drug discovery and development for neglected parasitic diseases. *Nat. Chem. Biol. 2*, 701−710.

(9) Eakin, A. E., Mills, A. A., Harth, G., McKerrow, J. H., and Craik, C. S. (1992) The sequence, organization, and expression of the major cysteine protease (cruzain) from *Trypanosoma cruzi*. *J. Biol. Chem. 267*, 7411−7420.

DOI: 10.1021/bi501551g
Biochemistry 2015, 54, 3381−3391

(10) Itow, S., and Camargo, E. P. (1977) Proteolytic activities in cell-extracts of *Trypanosoma cruzi*. *J. Protozool. 24*, 591−595.
(11) Campetella, O., Henriksson, J., Aslund, L., Frasch, A. C. C., Pettersson, U., and Cazzulo, J. J. (1992) The major cysteine proteinase (Cruzipain) from *Trypanosoma cruzi* is encoded by multiple polymorphic tandemly organized genes located on different chromosomes. *Mol. Biochem. Parasitol. 50*, 225−234.
(12) Fujii, N., Mallari, J. P., Hansell, E. J., Mackey, Z., Doyle, P., Zhou, Y. M., Gut, J., Rosenthal, P. J., McKerrow, J. H., and Guy, R. K. (2005) Discovery of potent thiosemicarbazone inhibitors of rhodesain and cruzain. *Bioorg. Med. Chem. Lett. 15*, 121−123.
(13) Scharfstein, J., Schechter, M., Senna, M., Peralta, J. M., Mendoncapreviato, L., and Miles, M. A. (1986) *Trypanosoma cruzi* characterization and isolation of a 57/51,000 MW surface glycoprotein (GP57/51) expressed by epimastigotes and blood-stream trypomastigotes. *J. Immunol. 137*, 1336−1341.
(14) Schnapp, A. R., Eickhoff, C. S., Sizemore, D., Curtiss, R., and Hoft, D. F. (2002) Cruzipain induces both mucosal and systemic protection against *Trypanosoma cruzi* in mice. *Infect. Immun. 70*, 5065−5074.
(15) Cazzulo, J. J. (2002) Proteinases of *Trypanosoma cruzi*: Potential targets for the chemotherapy of Changas desease. *Curr. Top. Med. Chem. 2*, 1261−1271.
(16) Cazzulo, J. J., Stoka, V., and Turk, V. (1997) Cruzipain, the major cysteine proteinase from the protozoan parasite *Trypanosoma cruzi*. *Biol. Chem. 378*, 1−10.
(17) Engel, J. C., Doyle, P. S., Hsieh, I., and McKerrow, J. H. (1998) Cysteine protease inhibitors cure an experimental *Trypanosoma cruzi* infection. *J. Exp. Med. 188*, 725−734.
(18) Engel, J. C., Doyle, P. S., Palmer, J., Hsieh, I., Bainton, D. F., and McKerrow, J. H. (1998) Cysteine protease inhibitors alter Golgi complex ultrastructure and function in *Trypanosoma cruzi*. *J. Cell Sci. 111*, 597−606.
(19) Harth, G., Andrews, N., Mills, A. A., Engel, J. C., Smith, R., and McKerrow, J. H. (1993) Peptide-fluoromethyl ketones arrest intracellular replication and intercellular transmission of *Trypanosoma cruzi*. *Mol. Biochem. Parasitol. 58*, 17−24.
(20) McKerrow, J. H. (1999) Development of cysteine protease inhibitors as chemotherapy for parasitic diseases: Insights on safety, target validation, and mechanism of action. *Int. J. Parasitol. 29*, 833−837.
(21) Polticelli, F., Zaini, G., Bolli, A., Antonini, G., Gradoni, L., and Ascenzi, P. (2005) Probing the cruzain S-2 recognition subsite: A kinetic and binding energy calculation study. *Biochemistry 44*, 2781−2789.
(22) Barr, S. C., Warner, K. L., Kornreic, B. G., Piscitelli, J., Wolfe, A., Benet, L., and McKerrow, J. H. (2005) A cysteine protease inhibitor protects dogs from cardiac damage during infection by *Trypanosoma cruzi*. *Antimicrob. Agents Chemother. 49*, 5160−5161.
(23) Brak, K., Doyle, P. S., McKerrow, J. H., and Ellman, J. A. (2008) Identification of a new class of nonpeptidic inhibitors of cruzain. *J. Am. Chem. Soc. 130*, 6404−6410.
(24) Doyle, P. S., Zhou, Y. M., Engel, J. C., and McKerrow, J. H. (2007) A cysteine protease inhibitor cures Chagas' disease in an immunodeficient-mouse model of infection. *Antimicrob. Agents Chemother. 51*, 3932−3939.
(25) Jacobsen, W., Christians, U., and Benet, L. Z. (2000) In vitro evaluation of the disposition of a novel cysteine protease inhibitor. *Drug Metab. Dispos. 28*, 1343−1351.
(26) Roush, W. R., Cheng, J. M., Knapp-Reed, B., Alvarez-Hernandez, A., McKerrow, J. H., Hansell, E., and Engel, J. C. (2001) Potent second generation vinyl sulfonamide inhibitors of the trypanosomal cysteine protease cruzain. *Bioorg. Med. Chem. Lett. 11*, 2759−2762.
(27) Otto, H. H., and Schirmeister, T. (1997) Cysteine proteases and their inhibitors. *Chem. Rev. 97*, 133−171.
(28) Lecaille, F., Kaleta, J., and Bromme, D. (2002) Human and parasitic papain-like cysteine proteases: Their role in physiology and pathology and recent developments in inhibitor design. *Chem. Rev. 102*, 4459−4488.
(29) Schoellmann, G., and Shaw, E. (1963) Direct evidence for presence of histidine in active center of chymotrypsin. *Biochemistry 2*, 252−255.
(30) Rasnick, D. (1985) Systhesis of peptide fluoromethyl ketones and the inhibition of human cathepsin-B. *Anal. Biochem. 149*, 461−465.
(31) Rauber, P., Angliker, H., Walker, B., and Shaw, E. (1986) The synthesis of peptidylfluoromethanes and their properties as inhibitors of serine proteinases and cysteine proteinases. *Biochem. J. 239*, 633−640.
(32) Gillmor, S. A., Craik, C. S., and Fletterick, R. J. (1997) Structural determinants of specificity in the cysteine protease cruzain. *Protein Sci. 6*, 1603−1611.
(33) McGrath, M. E., Eakin, A. E., Engel, J. C., McKerrow, J. H., Craik, C. S., and Fletterick, R. J. (1995) The crystal structure od cruzain: A therapeutic target for Chagas disease. *J. Mol. Biol. 247*, 251−259.
(34) Gilles, A. M., and Keil, B. (1984) Evidence for an active-center cysteine in the SH-proteinase α-clostripan through use of N-tosyl-L-lysine chloromethyl ketone. *FEBS Lett. 173*, 58−62.
(35) Polgar, L. (1973) Mode of activation of catalytically essential sulfhydryl group of papain. *Eur. J. Biochem. 33*, 104−109.
(36) Polgar, L., and Halasz, P. (1982) Current problems in mechanistic studies of serine and cysteine proteinases. *Biochem. J. 207*, 1−10.
(37) Keillor, J. W., and Brown, R. S. (1992) Attack of zwitterionic ammonium thiolates on a distorted anilide as a model for the acylation of papain by amides: A simple demonstration of a bell-shaped pH rate profile. *J. Am. Chem. Soc. 114*, 7983−7989.
(38) Brocklehurst, K. (1979) Specific covalent modification of thiols: Applications in the study of enzymes and other biomolecules. *Int. J. Biochem. 10*, 259−274.
(39) Arafet, K., Ferrer, S., Martí, S., and Moliner, V. (2014) Quantum Mechanics/Molecular Mechanics Studies of the Mechanism of Falcipain-2 Inhibition by the Epoxysuccinate E64. *Biochemistry 53*, 3336−3346.
(40) Barreiro, G., deAlencastro, R. B., and Neto, J. D. D. (1997) A semiempirical study on leupeptin: An inhibitor of cysteine proteases. *Int. J. Quantum Chem. 65*, 1125−1134.
(41) Mendez-Lucio, O., Romo-Mancillas, A., Medina-Franco, J. L., and Castillo, R. (2012) Computational study on the inhibition mechanism of cruzain by nitrile-containing molecules. *J. Mol. Graphics Modelling 35*, 28−35.
(42) Mladenovic, M., Ansorg, K., Fink, R. F., Thiel, W., Schirmeister, T., and Engels, B. (2008) Atomistic insights into the inhibition of cysteine proteases: First QM/MM calculations clarifying the stereoselectivity of epoxide-based inhibitors. *J. Phys. Chem. B 112*, 11798−11808.
(43) Shankar, R., Kolandaivel, P., and Senthilkumar, K. (2010) Reaction Mechanism of Cysteine Proteases Model Compound HSH with Diketone Inhibitor $PhCOCOCH_3$-nXn, (X = F, Cl, n = 0, 1, 2). *Int. J. Quantum Chem. 110*, 1660−1674.
(44) Tarnowska, M., Oldziej, S., Liwo, A., Kania, P., Kasprzykowski, F., and Grzonka, Z. (1992) MNDO study of the mechanism of the inhibition of cysteine proteinases by diazomethyl ketones. *Eur. Biophys. J. 21*, 217−222.
(45) Vicik, R., Helten, H., Schirmeister, T., and Engels, B. (2006) Rational design of aziridine-containing cysteine protease inhibitors with improved potency: Studies on inhibition mechanism. *ChemMedChem 1*, 1021−1028.
(46) Vijayakumar, S., and Kolandaivel, P. (2008) Reaction mechanism of HSH and CH_3SH with $NH_2CH_2COCH_2X$ (X = F and Cl) molecules. *Int. J. Quantum Chem. 108*, 927−936.
(47) Powers, J. C., Asgian, J. L., Ekici, O. D., and James, K. E. (2002) Irreversible inhibitors of serine, cysteine, and threonine proteases. *Chem. Rev. 102*, 4639−4750.

DOI: 10.1021/bi501551g
Biochemistry 2015, 54, 3381−3391

(48) Arad, D., Langridge, R., and Kollman, P. A. (1990) A simulation of the sulfur attack in the cataliytic pathway of papain using molecular mechanics and semiempirical quantum-mechanics. *J. Am. Chem. Soc. 112*, 491−502.
(49) Howard, A. E., and Kollman, P. A. (1988) OH-versus-SH nucleophilic attack on amides: Dramatically different gas-phase and solvation energetics. *J. Am. Chem. Soc. 110*, 7195−7200.
(50) Han, W. G., Tajkhorshid, E., and Suhai, S. (1999) QM/MM study of the active site of free papain and of the NMA-papain complex. *J. Biomol. Struct. Dyn. 16*, 1019−1032.
(51) Byun, K., and Gao, J. L. (2000) A combined QM/MM study of the nucleophilic addition reaction of methanethiolate and N-methylacetamide. *J. Mol. Graphics Modelling 18*, 50−55.
(52) Strajbl, M., Florian, J., and Warshel, A. (2001) Ab initio evaluation of the free energy surfaces for the general base/acid catalyzed thiolysis of formamide and the hydrolysis of methyl thiolformate: A reference solution reaction for studies of cysteine proteases. *J. Phys. Chem. B 105*, 4471−4484.
(53) Wei, D. H., Huang, X. Q., Liu, J. J., Tang, M. S., and Zhan, C. G. (2013) Reaction Pathway and Free Energy Profile for Papain-Catalyzed Hydrolysis of N-Acetyl-Phe-Gly 4-Nitroanilide. *Biochemistry 52*, 5145−5154.
(54) Warshel, A., and Levitt, M. (1976) Theoretical studies of enzymic reactions: Dielectric, electrostatic and steric stabilization of carbonium-ion reaction lysozyme. *J. Mol. Biol. 103*, 227−249.
(55) Field, M. J., Bash, P. A., and Karplus, M. (1990) A combined quantum-mechanical and molecular mechanical potential for molecular-dynamics simulations. *J. Comput. Chem. 11*, 700−733.
(56) Gao, J. L., Amara, P., Alhambra, C., and Field, M. J. (1998) A generalized hybrid orbital (GHO) method for the treatment of boundary atoms in combined QM/MM calculations. *J. Phys. Chem. A 102*, 4714−4721.
(57) Field, M. J., Albe, M., Bret, C., Proust-De Martin, F., and Thomas, A. (2000) The Dynamo library for molecular simulations using hybrid quantum mechanical and molecular mechanical potentials. *J. Comput. Chem. 21*, 1088−1100.
(58) Bas, D. C., Rogers, D. M., and Jensen, J. H. (2008) Very fast prediction and rationalization of pK_a values for protein-ligand complexes. *Proteins: Struct., Funct., Bioinf. 73*, 765−783.
(59) Li, H., Robertson, A. D., and Jensen, J. H. (2005) Very fast empirical prediction and rationalization of protein pK_a values. *Proteins: Struct., Funct., Bioinf. 61*, 704−721.
(60) Olsson, M. H. M., Sondergaard, C. R., Rostkowski, M., and Jensen, J. H. (2011) PROPKA3: Consistent Treatment of Internal and Surface Residues in Empirical pK_a Predictions. *J. Chem. Theory Comput. 7*, 525−537.
(61) www.pymol.org (2009).
(62) Nam, K., Cui, Q., Gao, J., and York, D. M. (2007) Specific reaction parametrization of the AM1/d Hamiltonian for phosphoryl transfer reactions: H, O, and P atoms. *J. Chem. Theory Comput. 3*, 486−504.
(63) Jorgensen, W. L., Maxwell, D. S., and TiradoRives, J. (1996) Development and testing of the OPLS all-atom force field on conformational energetics and properties of organic liquids. *J. Am. Chem. Soc. 118*, 11225−11236.
(64) Jorgensen, W. L., Chandrasekhar, J., Madura, J. D., Impey, R. W., and Klein, M. L. (1983) Comparison of simple potential functions for simulating liquid water. *J. Chem. Phys. 79*, 926−935.
(65) Singh, U. C., and Kollman, P. A. (1986) A combined abinitio quantum-mechanical and molecular mechanical method for carrying out simulations on complex molecular systems: Applications to the $CH_3Cl + Cl^-$ exchange reaction and gas-phase protonation of polyethers. *J. Comput. Chem. 7*, 718−730.
(66) Martí, S., Moliner, V., and Tuñón, I. (2005) Improving the QM/MM description of chemical processes: A dual level strategy to explore the potential energy surface in very large systems. *J. Chem. Theory Comput. 1*, 1008−1016.
(67) Kumar, S., Bouzida, D., Swendsen, R. H., Kollman, P. A., and Rosenberg, J. M. (1992) The weighted histogram analysis method for free-energy calculations on biomolecules. 1. The method. *J. Comput. Chem. 13*, 1011−1021.
(68) Torrie, G. M., and Valleau, J. P. (1977) Non-physical sampling distributions in Monte Carlo free-energy estimation: Umbrella sampling. *J. Comput. Phys. 23*, 187−199.
(69) Ruiz-Pernia, J. J., Silla, E., Tuñón, I., Martí, S., and Moliner, V. (2004) Hybrid QM/MM potentials of mean force with interpolated corrections. *J. Phys. Chem. B 108*, 8427−8433.
(70) Chuang, Y. Y., Corchado, J. C., and Truhlar, D. G. (1999) Mapped interpolation scheme for single-point energy corrections in reaction rate calculations and a critical evaluation of dual-level reaction path dynamics methods. *J. Phys. Chem. A 103*, 1140−1149.
(71) Zhao, Y., and Truhlar, D. G. (2008) The M06 suite of density functionals for main group thermochemistry, thermochemical kinetics, noncovalent interactions, excited states, and transition elements: Two new functionals and systematic testing of four M06-class functionals and 12 other functionals. *Theor. Chem. Acc. 120*, 215−241.
(72) Hehre, W. J., Radom, L., von R. Schleyer, P., and Pople, J. (1986) *Ab Initio Molecular Orbital Theory*, John Wiley & Sons, New York.
(73) Lynch, B. J., Zhao, Y., and Truhlar, D. G. (2003) Effectiveness of Diffuse Basis Functions for Calculating Relative Energies by Density Functional Theory. *J. Phys. Chem. A 107*, 1384−1388.
(74) Frisch, M. J., Pople, J. A., and Binkley, J. S. (1984) Self-Consistent Molecular-Orbital Methods. 25. Supplementary functions for Gaussian-Basis Sets. *J. Chem. Phys. 80*, 3265−3269.
(75) Krishnan, R., Binkley, J. S., Seeger, R., and Pople, J. A. (1980) Self-Consistent Molecular-Orbital Methods. 20. Basis set for correlated wave-functions. *J. Chem. Phys. 72*, 650−654.
(76) Frisch, M. J., Trucks, G. W., Schlegel, H. B., Scuseria, G. E., Robb, M. A., Cheeseman, J. R., Scalmani, G., Barone, V., Mennucci, B., Petersson, G. A., Nakatsuji, H. C., Li, X., Hratchian, H. P., Izmaylov, A. F., Bloino, J., Zheng, G., Sonnenberg, J. L., Hada, M., Ehara, M., Toyota, K., Fukuda, R., Hasegawa, J., Ishida, M., Nakajima, T., Honda, Y., Kitao, O., Nakai, H., Vreven, T., Montgomery, J. A., Jr., Peralta, J. E., Ogliaro, F., Bearpark, M., Heyd, J. J., Brothers, E., Kudin, K. N., Staroverov, V. N., Kobayashi, R., Normand, J., Raghavachari, K., Rendell, A., Burant, J. C., Iyengar, S. S., Tomasi, J., Cossi, M., Rega, N., Millam, N. J., Klene, M., Knox, J. E., Cross, J. B., Bakken, V., Adamo, C., Jaramillo, J., Gomperts, R., Stratmann, R. E., Yazyev, O., Austin, A. J., Cammi, R., Pomelli, C., Ochterski, J. W., Martin, R. L., Morokuma, K., Zakrzewski, V. G., Voth, G. A., Salvador, P., Dannenberg, J. J., Dapprich, S., Daniels, A. D., Farkas, Ö., Foresman, J. B., Ortiz, J. V., Cioslowski, J., and Fox, D. J. (2009) *Gaussian 09*, revision A.1, Gaussian, Inc., Wallingford, CT.
(77) Rawlings, N. D., Barrett, A. J., and Bateman, A. (2012) MEROPS: The database of proteolytic enzymes, their substrates and inhibitors. *Nucleic Acids Res. 40*, D343−D350.
(78) Malthouse, J. P. G., Mackenzie, N. E., Boyd, A. S. F., and Scott, A. I. (1983) Detection of a tetrahedral adduct in a trypsin-chloromethyl ketone specific inhibitor complex by C-13 NMR. *J. Am. Chem. Soc. 105*, 1685−1686.

DOI: 10.1021/bi501551g
Biochemistry 2015, 54, 3381−3391